In vivo Antimalarial Activity of the Hydroalcoholic Extract of *Kniphofia foliosa* Hochst and Its Constituents

Yonatan Alebachew
Addis Ababa University College of Health Sciences https://orcid.org/0000-0002-9818-9168
Daniel Bisrat
Addis Ababa University College of Health Sciences
Solomon Tadesse
Addis Ababa University College of Health Sciences
Kaleab Asres (kaleab.asres@aau.edu.et)
Addis Ababa University College of Health Sciences https://orcid.org/0000-0003-1212-8688

Research

Keywords: Kniphofia foliosa, antimalarial activity, phenolic fractions, knipholone, dianellin

Posted Date: September 23rd, 2020

DOI: https://doi.org/10.21203/rs.3.rs-79326/v1

Version of Record: A version of this preprint was published at Malaria Journal on January 1st, 2021. See the published version at https://doi.org/10.1186/s12936-020-03552-7.

Abstract

Background: *Kniphofia foliosa* Hochst is endemic to Ethiopian highlands, where its rhizomes are traditionally used for the treatment of malaria, abdominal cramps and wound healing. As a continuation of our search for antimalarial compounds from Ethiopian medicinal plants, we have tested the 80% methanol extract of *K. foliosa* rhizomes and its constituents against *Plasmodium berghei* in mice.

Methods: Isolation was carried out using column and preparative thin layer chromatography (PTLC). The chemical structures of the compounds were elucidated by spectroscopic methods (ESI-MS, 1D and 2D-NMR). Peters' 4-day suppressive test against *P. berghei* in mice was utilized for *in vivo* antimalarial evaluation of the test substances.

Results: Three compounds, namely knipholone, dianellin, and 12-hydroxypentadec-9-en-1-yl methyl phthalate (HPMP) were isolated and characterized from the 80% methanolic extract of *K. foliosa* rhizomes. The *hydroalcoholic extract (*400 mg/kg) *and knipholone (*200 mg/kg) showed the highest activity with chemosuppression values of 61.52 and 60.16%, respectively. From the dose-response plot, the median effective (ED_{50}) doses of knipholone and dianellin were determined to be 81.25 and 92.31 mg/kg, respectively. Molecular docking study revealed that knipholone had a strong binding affinity to *Plasmodium falciparum* l-lactate dehydrogenase (pfLDH) target.

Conclusion: Results of the current study support the traditional use of the plant for the treatment of malaria.

Background

Malaria is one of the most serious life-threatening infectious diseases [1]. It occurs mostly in poor tropical and subtropical areas of the world, where the Africa region accounted for 93% of all malaria cases and 93.8% of malaria deaths [2]. Most often, pregnant women and children under five years old are severely affected [3]. For instance, from the total deaths due to malaria in 2018, 67% or 272,000 were children under 5 years of age. That is nearly 745 children under age 5 daily or one child under five every two minutes dies of malaria in 2018 alone and most of these deaths occurred in Sub-Saharan Africa [2]. In addition to funding shortfalls and fragile health systems, the major contributor to malarial morbidity and mortality is almost certainly the increasing resistance of malaria parasites to available drugs [4].

In Ethiopia, there has been success in the past recent years to reduce malaria burden. However, it is still prevalent in 75% of the country putting over 40 million people at risk [5]. The disease accounts for 7% of outpatient visits to health clinics and represents the third largest cause of morbidity [6]. In addition, 8% of global *Plasmodium vivax* malaria cases occur in Ethiopia [2]. Hence, the fight against malaria in Ethiopia remains a public health priority.

Natural products from plants have played a huge role throughout history in the fight against malaria. For instance, the aqueous extracts of cinchona bark were an effective antimalarial preparation for more than

300 years. Later, quinine, the major active alkaloid of cinchona was isolated in the 1820s. Similarly, artemisinin was isolated from the cold ether extracts of the leaves of Chinese traditional medicinal herb, *Artemisia annua* in 1972 [7]. Inspired by these, different classes of antimalarial compounds were isolated from a variety of plant families. Although hundreds of potent antimalarial compounds were isolated from African traditional medicine, there hasn't been any clinically successful molecule [8, 9, 10].

The genus *Kniphofia* belongs to the family Asphodelaceae which comprises 70 species mainly confined to Africa [11]. Fifteen of these species have been recorded in Eastern Africa, of which five including *Kniphofia foliosa* Hochst. are endemic to Ethiopia [12, 13]. The rhizomes of *K. foliosa* are traditionally used for the treatment of abdominal cramps, malaria and wounds [14]. Previously, six *in vitro* active antimalarial compounds were isolated from roots of *K. foliosa* by Wube *et al.* [15] and Abdissa *et al.* [16]. In our continued search for lead antimalarial compounds from Ethiopian medicinal plants [17, 18, 19], we have investigated the *in vivo* antimalarial activity of the rhizomes *K. foliosa* and its constituents.

Methods

Chemicals and instruments

Chromatographic separation were performed by analytical TLC on Silica gel 60 F254 (0.2 mm thick), column chromatography on Silica gel 60 (70–240 mesh) (Merck KGaA, Darmstadt, Germany) and solid phase separation on Isolute C_{18} columns (10 g; IST, Hengoed, UK). Trisodium citrate was obtained from BDH Chemicals Ltd, England, Geimsa stain was purchased from ESJAY Chemicals, Maharashtra 401504, India, and pure chloroquine phosphate was supplied by Ethiopian Pharmaceutical Manufacturing Factory (EPHARM, Ethiopia).

NMR spectra were recorded at 500 MHz for ^{1}H and 125 MHz for ^{13}C on a Bruker Avance DMX400 FT-NMR spectrometer (Bruker, Billerica, Massachusetts, USA) using tetramethylsilane (TMS) as internal standard. All spectra were measured in $CDCl_3$, except for compounds **1**, which was dissolved in CD_3OD. HRMS were determined on a Shimadzu LC-MS Advanced spectrometer (Shimadzu, Kyoto, Japan) in the positive and negative modes.

Plant material

The rhizomes of *K. foliosa* were collected in February 2017 from mount Kundi near the city of Ankober in Shewa region of Central Ethiopia and identified by Professor Sebsibe Demisew at the National Herbarium, Addis Ababa University (AAU), Addis Ababa, Ethiopia, where voucher specimens were deposited (Collection number: YA01/2017).

Experimental animals

Healthy, 5–6 weeks old Swiss albino mice of either sex weighing 20–25 g were employed throughout the experiment. Most of the mice were obtained from the animal house of the School of Pharmacy (SoP), AAU, and the rest were purchased or gifted, respectively, from the Ethiopian Health Nutrition and Research Institute (EHNRI) and Rift Valley Health Science College, Addis Ababa. The animals were held in stainless steel cages at room temperature and relative humidity for12 hour light-dark cycle. They were provided with food and water *ad libitum* in the animal house of the SoP, College of Health Sciences, AAU. They were acclimatized for one week before the experiment.

Rodent parasite

Chloroquine (CQ) sensitive strain of *Plasmodium berghei* ANKA strain was used. The donor mice infected with the parasite was obtained from the EHNRI. The parasites were maintained by serial blood passage from mouse to mouse at 5 days interval. All procedures followed were in accordance with the Guide for the Care and Use of Laboratory Animals [20] and were approved by the Institutional Review Board of the SoP, College of Health Sciences, AAU.

Extraction, fractionation and isolation

The air-dried powdered rhizomes of *K. foliosa* were soaked in 80% methanol at room temperature for 4 days with occasional shaking. Removal of the organic solvent using rotary evaporator (BUCHI Rotavapor™ R-300, Switzerland) followed by freeze drying of the remaining water extract yielded a dark red gummy solid. Portion of the dried extract was dissolved in 5% KOH solution and partitioned with chloroform. The aqueous phase was acidified with 2% HCl and then further partitioned with chloroform. The chloroform layer was collected and concentrated in a rotavapor to give a dried solid designated crude phenolic fraction I. The reddish solid mass (methanol soluble) formed between the acidified aqueous and chloroform layers was collected as phenolic fraction II. Purification of phenolic fraction I by preparative TLC and column chromatography, respectively (Supplementary Fig. 1) gave KFP-1 and KFP-5. Furthermore, portion of the hydroalcoholic extract was fractionated on silicagel flash column chromatography to yield three fractions. Fraction 1 was eluted with 100% chloroform, fractions 2 and 3 with a mixture of chloroform and methanol (1:1), and fraction 4 with 100% methanol. Fraction 3 was concentrated and freeze dried to give viscous solid, which was further purified by sequential PTLC and solid phase extraction on Isolute C_{18} columns to give YKFM-2 (Supplementary Fig. 2).

Acute oral toxicity testing

Acute oral toxicity study was conducted as per the internationally accepted protocol of OECD Guideline 425 [21]. Ten healthy Swiss female albino mice weighing 20–25 g were randomly grouped into 2 each having 5 mice (A to E). Following 3–4 h of fasting (with food only), one mouse from each group was orally administered 2000 mg/kg of the hydroalcoholic extract and KFP-1, respectively. The mice were then

observed individually for any physical or behavioral changes such as loss of appetite, hair erection, lacrimation, mortality, and other signs of toxicity for 4 h. The same procedure was followed for the remaining mice for the next five consecutive days and the results recorded. The follow-up observations was continued for all mice for 14 days.

In vivo antimalarial assay

Inoculation

Blood smear was prepared on microscope slides from blood films taken from the donor (infected) mouse tail. The smear was fixed with methanol and stained with Giemsa to count the parasitemia of the donor under a microscope. The mice were then inoculated on day 0 with parasitized erythrocytes obtained from the donor by cardiac puncture using a sterile syringe when the parasitaemia level was 30–40%. The blood from the donor was collected on a Petri dish containing 2% trisodium citrate and was immediately diluted with uninfected mouse blood and normal saline in such way that the final volume contains 5×10^7 infected erythrocytes/ml of blood. The diluted blood (0.2 ml) was injected into all the experimental mice intraperitoneally [22, 23].

4–Day suppressive test

The standard 4-day suppressive method was used for antimalarial evaluation of the test substances. The test was carried out in two phases. The extract and phenol fractions were evaluated in the first phase followed by KFP-1 and YKFM-2 in the second phase. During the first phase, 60 inoculated mice were randomly grouped into 12 groups each having five mice. Groups 1 served as a negative control (distilled water,Vehicle1, 0.2 ml) for the extract and phenolic fraction 2 treated groups, while group 2 animals were used as a negative control (1% tween 80, Vehicle2, 0.2 ml) for phenolic fraction 1 treated group. The third group which served as a positive control was treated with standard pure chloroquine (25 mg/kg/day). The remaining nine groups were treatment groups and received 100, 200, and 400 mg/kg/day of the hydroalcoholic extract and the two phenol fractions. Similarly, during evaluation of KPF-1 and YKFM-2, 45 inoculated mice were randomly grouped into 9 groups, each containing five mice. The first two groups were negative controls (distilled water, Vehecle3, 0.2 ml) and positive controls (standard pure chloroquine, 25 mg/kg/day). The rest of the groups were treatment groups and received KFP-1 or YKFM-2 at doses of 25, 50, 100 and 200 mg/kg/day. All the test substances were administered orally using oral gavage. Treatment was started 3 h post-infection on day 0 and continued daily for the next 3 days (i.e. from day 0 to day 3). On the fifth day (or day 4), two Giemsa-stained blood smears were prepared from each mice to count the number of parasites under the microscope with an oil immersion objective of 100x magnification power [24, 25, 26].

Mean percent parasitaemia and percent suppression were calculated using the following formulae.

$$\% \text{ Parasitemia } = \left(\frac{\text{Number of parasitized RBC}}{\text{Total number of RBC count}}\right) X\, 100$$

$$\% \text{ Suppression } = \left(\frac{\text{Mean parasitemia of negative control} - \text{ Mean parasitemia of treated}}{\text{Mean parasitemia of negative control}}\right) X\ 100$$

Body weight and survival time measurement

Body weight of each mouse was measured on day 0 before infection and on day 4. Survival time was recorded from day 1 to day 28 post inoculation. Then, mean body weight and mean survival time were calculated for each group [19].

Molecular docking study

Docking study was carried out on two crystal structures of *plasmodium* enzymes plasmepsin II (Protein Data Bank; PDB: 4CKU) and l-lactate dehydrogenase (pfLDH) [PDB: 1LDG], using SeeSar10.0 software (BioSolveIT, Sankt Augustin, Germany). For plasmepsin II, the selected binding site was the binding pocket of a previously designed inhibitor P2FE-400, while for pfLDH, the cofactor nicotinamide adenine dinucleotide (NADH) binding site was selected for docking. The HYDE score was used to estimate the binding affinity of the molecules [27, 28].

Statistical analysis

Data analysis was carried out using IBM SPSS (Statistical Package for Social Sciences) Statistics for Windows, Version 20.0. Armonk, NY: IBM Corp. Results were expressed as mean ± standard error of mean (M ± SEM). The statistical significance was determined by one-way ANOVA followed by Tukey post hoc test to compare percent suppression (activity), mean survival time and percent changes in body weight of the *P. berghei* infected mice among the treatment and control groups. $P < 0.05$ were considered significant.

Results And Discussion

Structural elucidation of the isolated compounds

Phytochemical investigation of the rhizome extract of *K. folosia* over silcagel column and PTLC resulted in the isolation of three compounds with R_f values of 0.69 (YKFM-2; **1** [BAW/EtOAc; 1:1]), 0.47 (KFP-1; **2** [Toluene/EtOAc; 5:1]) and 0.62 (KFP-5; **3** [Hexane/EtOAC; 3:1]).

Compound **1** was obtained as a light red amorphous solid. The positive high resolution-ESI mass spectrum gave a pseudomolecular ion at *m/z* 547.1619 $[M + Na]^+$ (calcd. *m/z* 547.1791 $[M + Na]^+$, corresponding to a molecular formula $C_{25}H_{32}O_{12}$. In the ^1H NMR spectrum, four proton signals which resonated at δ 7.12 (*s*, H-4), 7.52 (*m*, H-7), 7.62 (*m*, H-6) and 7.62 (*m*, H-5) indicated the presence of aromatic ring moiety. Moreover, three of these proton signals which are multiplets imply that they are found in close proximity (or are adjacent) and the fourth singlet aromatic proton peak at δ 7.12 (*s*, H-4) provides clues for the presence of a fused aromatic ring system. The presence of a disaccharide unit in compound **1** was revealed by the typical anomeric proton signals at δ 4.28 (d, *J* = 3.2 Hz, 1H, H-4") and 5.25 (d, *J* = 3.7 Hz, 1H, H-1'). The proton peaks from δ 5.25 to 3.06 further justify the presence of a disaccharide moiety. The ^{13}C spectrum region from δ 76.82 to 66.59 also confirmed that the compound contains a disaccharide moiety. In addition, the two elevated ^{13}C sugar signals at δ 102.84 and 100.85 indicate that the sugar units are linked through acetal bond. Furthermore, the absence of one CH signal in the sugar region (δ 76.82 - δ 66.59) suggests one of the sugar units to be rhamnose. And this was found to be in good agreement with ^{13}C NMR reports of similar glycosides [29, 30]. Hence, the disaccharide moiety was confirmed to be rhamnose-glucose 1,6 linkage. In addition, the presence of 10 ^{13}C signals from δ 154.71 to δ 110.5 implies that the fused aromatic ring system is naphthalene. Six of these carbon signals are absent from DEPT spectrum indicating they are quaternary aromatic carbons. Besides, two of them are elevated (δ 154.71 and δ 151.49) suggesting that they are oxygenated quaternary aromatic carbons. On the other hand, the two less elevated (δ 136.74 and δ 113.54) quaternary aromatic carbons are the bridgehead carbons of the fused aromatic system [30]. The remaining two quaternary aromatic carbon signals resonated at δ 124.73 (C-2) and δ 133.30 (C-3). Lastly, the ^{13}C signals at 207.7 and 41.3 are the carbonyl carbon and its acetyl methyl. Therefore, based on the above evidence and in comparison with ^1H and ^{13}C NMR data of the same and related compounds [30, 31], the structure of compound **1** was determined to be dianellin or 1-(1-hydroxy-3-methyl-8-(((2S,3R,4S,5S,6R)3,4,5-trihydroxy-6-((((2S,3S,4S,5S,6R)3,4,5-trihydroxy-6-methyltetrahydro-2H-pyran-2-yl)oxy)methyl)tetrahydro-2H-pyran-2yl)oxy)naphthalen-2-yl) ethanone. Table 1 summarizes the NMR data of compound **1**.

Table 1

^{1}H and ^{13}C NMR data of compound **1** measured in methanol-d_4.

Present data			Reference data [31]	
Position	δ_C (ppm)	δ_H(ppm)	δ_C (ppm)	δ_H(ppm)
1	151.49	-	150.2	-
2	124.73	-	125.2	-
3	133.30	-	132.8	-
4	119.58	7.12 (1H, *s*)	119.4	7.21 (1H, *s*)
5	122.58	7.66 (1H, *m*)	122.3	7.47 (1H, *dd*, J = 1.0, 8.0 Hz)
6	127.20	7.62 (1H, *m*)	127.3	7.40 (1H, *dd*, J = 8.0, 8.0 Hz)
7	110.51	7.52 (1H, *m*)	110.7	7.30 (1H, *dd*, J = 1.0, 8.0 Hz)
8	154.71	-	154.2	-
9	113.54	-	113.2	-
10	136.74	-	135.7	-
1’	100.86	5.25 (*d*, *J* = 3.7 Hz, 1H)	102.6	5.04 (1H, *d*, J = 7.5 Hz)
2’	73.57	3.41 (*dd*, *J* = 11.3, 6.0 Hz, 1H)	73.3	3.39 (1H, *m*)
3’	76.82	3.35 (dt, *J* = 3.3, 1.7 Hz, 1H)	76.2	3.36 (1H, *m*)
4’	70.13	2.91 (d, *J* = 2.6 Hz, 1H)	70.1	3.18 (1H, *m*)
5’	76.10	3.59–3.55 (*m*, 1H)	76.0	3.59 (1H, *m*)
6	66.59	3.52–3.49 (*m*, 1H, H-6b’); 3.97 (dd, *J* = 6.6, 1.1 Hz, 1H, H-6a’)	66.6	3.93 (1H, *dd*, J = 1.5, 11.0 Hz); 3.50 (2H, *m*)
1”	102.84	4.28 (d, *J* = 3.2 Hz, 1H)	100.7	4.62 (1H, *d*, J = 1.5 Hz)
2”	70.84	3.89–3.85 (*m*, 1H)	70.4	3.68 (1H, *m*)
3”	71.03	3.51–3.49 (*m*, 1H)	70.7	3.50 (2H, *m*)
4”	72.59	3.06 (*m*, 1H)	71.9	3.20 (1H, *m*)
5”	68.55	3.47 (d, *J* = 1.8 Hz, 1H)	68.4	3.49 (1H, *m*)
6”	16.55	1.23 (*s*,3H)	17.7	1.12 (3H, *d*, J = 6 Hz)
$ArCH_3$	18.49	1.79 (*s*, 3H)	19.0	2.25 (3H, *s*)

Present data			Reference data [31]	
$COCH_3$	41.3	2.54 (*s*, 3H)	31.9	2.52 (3H, *s*)
$COCH_3$	207.07	-	204.4	-

Compound **2** was isolated as an orange colored amorphous solid. The molecular formula was determined to be $C_{24}H_{18}O_8$ by the positive-ion ESIMS spectrum (*m/z* 458.21 $[M + Na]^+$), which was also consistent with ^1H and ^{13}C NMR spectral data. The chelated hydroxyl protons shown as singlet peaks at δ 12.6 and 11.9 and the typical ABC pattern of the proton peaks at δ7.57 (H-6), 7.55 (H-5) 7.21 (H-7) indicate the presence of chrysophanol moiety. Besides, the singlet aromatic proton signal present at 7.28 suggests that it is found adjacent to a substituted aromatic carbon. The ^{13}C and DEPT spectra of compound **2** also support the presence of chrysophanol moiety [32, 33]. Moreover, from the ^{13}C spectrum, additional aromatic carbon signals at δ 151.6, 131.6, 128.5, 124.6, and 119.3 together with the ^1H peaks at 14.22 (s, OH), 6.24 (s, aromatic H), 5.6 (s (*br*), OH) and 3.98 (s, OCH_3) indicate the attachment of a methyl etherified acetylphloroglucinol moiety to chrysophanol. These data in comparison with the reported ^1H and ^{13}C NMR results identify compound **2** as knipholone.

Compound **3** was isolated as a yellow amorphous solid. It exhibited a pseudomolecular ion peak at *m/z* 427 $[M + Na]^+$ on the positive-ion ESIMS spectrum suggesting its molecular weight to be 404.54. The chemical formula $C_{24}H_{36}O_5$ was deduced for Compound **3** on the basis of ESIMS and NMR data. In the ^1H NMR spectrum, the four distinct aromatic proton signals (at δ 7.85, δ 7.69, δ 7.3, δ 7.12) denote the presence of a disubstituted aromatic ring. The peak at δ 3.7 is indicative of the presence of OCH_3 protons. The broad peak at δ 5.5 CH (SP^2) establishes the presence of double bond. In addition, there is an indication for OCH_2 (at δ 4.35a, 4.15b) and OH proton (at δ 5.13). The proton peak at δ 2.8 affirms the presence of OCH proton (also supported by ^{13}C). The other proton peaks in the upfield region between δ 2.3 and δ 0.89 are congested CH_2 peaks with the one at the end being CH_3 (δ 0.89). In the ^{13}C NMR spectrum, there are 8 signals between δ 135.17 and 127.09 in two sets, 6 of them are aromatic ring carbons and two are CH (SP^2) double bond carbons. Furthermore, the two carbonyl carbon peaks shown at δ 174.30 and δ 172.83 suggest the occurrence of esterified OCH_3 and long-chain alkane. This is clearly supported by the DEPT spectrum which shows a single OCH_2 peak at δ 62.08 and OCH_3 peak at δ 51.42, and the rest of the congested CH_2 carbon peaks are aligned as expected from δ 34.04 to δ 14.12 with peak at δ 14.12 assigned to CH_3 [34, 35, 36, 37]. Hence, based on the above data and in comparison with the ^1H NMR and ^{13}C NMR of related compounds, the structure of compound **3** was determined to be 12-hydroxypentadec-9-en-1-yl methyl phthalate (HPMP). Table 2 summarizes the NMR data of compounds **2** and **3**.

Table 2

^{1}Hand ^{13}C NMR data of compounds **2** and **3** in chloroform-*d.*

Compound 2 - present data			**Compound 2 - reference data [33]**		**Compound 3 - present data**		
Position	**δ_C (ppm)**	**δ_H (ppm)**	**δ_C (ppm)**	**δ_H (ppm)**	**Position**	**δ_C (ppm)**	**δ_H(ppm)**
1	161.69	12.6 (*s*, 1H,-OH)	161.7	12.53 (*s*, 1H,-OH)	1	14.12	0.89 (*s*, 3H)
1a	115.22	-	114.7	-	2	22.58	1.2-1.4 (*br, m*, 2H)
2	125.31	7.28 (*s*,1H)	124.6	7.32 *(qu, J* = 0.7 Hz	3	34.09	1.2-1.4(br, *m*, 2H)
3	152.44	-	151.6		4	68.86	2.8 (*br*,1H)
4	125.75	-	128.5		5	39.72	2.3 (*s*, 2H)
4a	132.72	-	131.6		6	129.88	5.5 (*br*, 1H)
5	120.11	7.55 (*dd*,1H)	119.3	7.56 (*dd*, *J* = 7, 1.5 Hz)	7	129.72	5.5 (*br*, 1H),
5a	134.27	-	134.4		8	32.19	2.11 (*s*, 2H)
6	137.12	δ7.57 (*dd*,1H)	137.4	7.75 (*dd*, *J* = 8, 7 Hz)	9	29.27	1.2-1.4(*br,m*, 2H)
7	123.85	7.21(*dd*,1H)	123.3	7.30 (*dd*, J = 8, 1.5 Hz)	10	29.16	1.2-1.4(*br, m*, 2H)
8	159.51	11.9 (*s*, 1H,-OH)	161.1	12.0 (*s*, 1H,-OH)	11	29.27	1.2-1.4(*br, m,* 2H)
8a	115.37	-	115.5	-	12	26.39	1.2-1.4(*br, m*, 2H)
9	192.68	-	192.5	-	13	25.61	1.2-1.4(*br, m,* 2H)
10	182.66	-	181.9	-	14	27.19	1.6 (*s*, 2H)
1’	106.07	-	104.7	-	15	62.86	4.35(a, 1H), 4.15 (b, 1H)
2’	163.27	5.7 (*s* (br), 1H,-OH)	163.3	8.95 (*s* (br))	1	135.17	-
3’	107.14	-	107.3	-	2	129.07	-
4’	163.07	-	162.4	-	3	128.26	7.85 (*m*, 1H)
5’	90.61	6.19 (*s*,1H)	91.2	6.24 (*s,* 1H)	4	130.01	7.3 (*m*, 1H)

6’	162.85	14.3 (*s*, 1H,-OH)	161.9	-	5	130.18	7.12 (*m*, 1H)
$ArCH_3$	21.02	2..21(*s*.3H)	20.4	2.17 (*d*, *J* = 0.7 Hz)	6	128.02	7.69 (*m*, 1H)
OCH_3	55.56	3.91(*s*,3H)	55.6	3.98 (*s*, 3H)	$CO\underline{CH_3}$	51.42	3.7 (*s*, 3H)
$CO\underline{CH_3}$	33.14	2.70(*s*,3H)	32.6	2.62 (*s*, 3H)	$\underline{C}OCH_3$	174.30	-
$\underline{C}OCH_3$	202.3	-	202.3	-	$\underline{C}OO$	173.26	-

Acute oral toxicity

Acute oral toxicity test results of this study documented that the 80% methanol extract of *K. foliosa* and knipholone were safe at a dose of 2000 mg/kg [21, 38]. After 72 hours, the animals tolerated the administered dose although immediate mild toxicity signs such as hair erection and loss of appetite, which disappeared few hours after administration were observed. Also, there was no mortality within 14 days of observation which entails that the LD_{50}s of the extract and knipholone are above 2000 mg/kg.

Antimalarial activity of the hydroalcoholic extract

The 80% methanol extract of *K. folosia* showed chemosuppressive effect against *P. berghei* in mice (Table 3). At all dose levels tested, the extract exhibited a statistically significant ($p < 0.001$) dose dependent effect. The extract showed the highest activity with 61.52 and 51.39% suppression at 200 and 400 mg/kg, respectively. Moreover, at doses of 200 and 400 mg/kg, the extract significantly extended the survival days of treated groups compared to the negative controls, indicating that the extract has the capacity to lower the overall pathologic effect of the parasite in mice. However, there was no significant difference in percent change in weight before and after treatment among groups except with the positive control group. According to Deharo *et al.* [39], antimalarial activity of the 80% methanol extract of *K. folosia* can be regarded as good since it showed greater than 50% suppression at a dose of 200 mg/kg. Previous studies demonstrated that medicinal plants rich in anthraquinones such as aloes and senna possess notable *in vivo* antimalarial activity [40, 41].

Table 3
Antimalarial activity of the 80% extracts of *K. folosia*in mice infected with *Plasmodium berghei*.

Test substances	Dose (mg/kg/day)	Percent parasitaemia	Percent Suppression	Mean survival time (in days)
Vehicle1	0.2 ml	35.9860 ± 1.22034	0.0000	6.0000 ± .31623
KF100	100 mg	24.2100 ± 1.18037	32.7200^{a*c**d*e*}	9.4000 ± 0.50990^{a**e*}
KF200	200 mg	17.4920 ± 0.67964	51.3900^{a*b**e*}	9.6000 ± 0.92736^{a*e*}
KF400	400 mg	13.8480 ± 0.76024	61.5200^{a*b*e*}	8.4000 ± 0.24495^{e*}
Chloroquine	25 mg	0.0140 ± 0.00600	99.8000^{a*b*c*d*e*f*g*h*}	27.2000 ± .58310^{a*b*c*d*}

Values are presented as mean ± SEM; n = 5; a = compared to vehicle1 (distilled water), b = compared to KF100, c = compared to KF200, d = compared to KF400, e = compared to chloroquine; * ($p < 0.001$); **($p < 0.01$); KF = 80% extracts of *K. folosia*, numbers refer to doses in mg/kg/day.

Antimalarial activity of the phenol fractions and their constituents

The two phenolic fractions of *K. folosia* were also found to have activity against *P. berghei* in mice (Fig. 2). Compared to their respective negative controls, both factions possessed significant suppressive activity at all dose levels tested. They showed the highest activity at 400 mg/kg with fraction 1 and fraction 2 causing 46.32% and 47.53% suppression, respectively. Both fractions prolonged the mean survival days of the treatment groups by 2 days relative to their negative controls although it was not statistically significant. No significant difference in percent change in weight was noted in the treatment groups when compared with the positive controls. Therefore, it can be deduced that the phenolic fractions of *K. folosia* are moderate in their *in vivo* antimalarial activity, congruent with earlier reports that extracts containing phenolic compounds and their glycosides have modest levels of antiplasmodial activity [42, 43, 44].

Among the isolated compounds, knipholone displayed the strongest antimalarial activity against *P. berghei* infected mice (Table 4). Although knipholone and dianellin showed significant suppression at all dose levels tested, the former displayed superior activity with percent suppression values of 51.5 and 61.5% at doses of 100 and 200 mg/kg, respectively. Moreover, it significantly prolonged the mean survival days of the treatment groups (Table 4). The dose-response plot (Fig. 3) disclosed that the ED_{50} values of knipholone and dianellin were 81.25 and 92.31 mg/kg, respectively. However, neither of the compounds caused significant difference in percent change of weight among the treated groups.

Table 4
Antimalarial activity of knipholone and dianellin in mice infected with *Plasmodium berghei*.

Test substances	Dose (mg/kg/day)	Percent Parasitaemia	Percent suppression	Mean survival time (in days)
Vehicle3	0.2 ml	46.3560 ± 1.46925	0.0000	6.4000 ± 0.50990
Knipholone	25 mg	30.5440 ± 1.45634	34.1200^{a*d*e*h*i*}	8.8000 ± 0.37417^{i*}
Knipholone	50 mg	26.2640 ± 1.80001	42.6400^{a*e**h*i*}	9.0000 ± 0.54772^{i*}
Knipholone	100 mg	20.7940 ± 0.91475	55.1400^{a*b*e**f*g*i*}	9.2000 ± 0.73485^{a***i*}
Knipholone	200 mg	18.4680 ± 0.97391	60.1600^{a*b*c**f*g*i*}	9.4000 ± 0.24495^{a**i*}
Dianellin	25 mg	32.5280 ± 0.96771	29.8300^{a*c*d*e*h*h*i*}	7.6000 ± 0.24495^{i*}
Dianellin	50 mg	25.9408 ± 0.77243	44.0400^{a*d*e*g*h*i*}	8.2000 ± 0.37417^{i*}
Dianellin	100 mg	21.4303 ± 0.84156	53.7700^{a*b*c*f*g*i*}	8.2000 ± 0.37417^{i*}
Chloroquine	25 mg	0.0140 ± .00600	99.8000^{a-h*}	27.4000 ± .400000^{a-h*}

Values are presented as mean ± SEM; n = 5; a = compared to vehicle3 (distilled water), b = compared to knipholone 25 mg, c = compared to knipholone 50 mg, d = compared to knipholone 100 mg, e = compared to knipholone 200 mg, f = compared to dianellin 25 mg, g = compared to dianellin 50 mg, h = compared to dianellin 100 mg, i = compared to chloroquine; * ($p < 0.001$); **($p < 0.01$); ***($p < 0.05$); numbers refer to doses in mg/kg/day.

Perusal of literature reveals that a number of promising anthraquinones and preanthraquinones leads such as visimione, rufigallol, uveoside, aloin and phenyl anthraquinones have been isolated and/or synthesized [15, 45, 46, 47]. These compounds are considered as oxidants like artemisinins and 4-aminoquinolines. More importantly, they are catalytic oxidants that enhance the production of reactive oxygen species (ROS) inside parasitized erythrocytes or increase these cells' susceptibility to oxygen radicals. The free oxygen radicals formed interact with heme or other biomolecular targets inhibiting its tetramerization to the insoluble hemozoin (malaria pigment) [48, 49]. Knipholone, being an anthraquinone derivative, is anticipated to undergo one-electron oxidation and subsequently interact with heme (or other biomolecular targets) thereby inhibiting its tetramerization (or detoxification of heme). Similarly, because of the structural similarity of dianellin with phlorizin, a monoglucosidechalcone, its antimalarial mechanism of action could be due to inhibition of the solute transporter of the host cell membrane induced by the parasite invasion [50, 51].

Molecular docking study

To get further insight on the mechanism of action of the isolated compounds and to study their binding interaction and identify hypothetical binding motifs, a docking study of **knipholone,** dianellin, HPMP and the standard antimalarial drugs chloroquine and artemisin were carried out on two crystal structures of enzymes. The two *Plasmodium* enzymes were plasmepsin II (PDB code 4cku) involved in haemoglobin metabolism by the parasite, and *P. falciparum* l-lactate dehydrogenase (pfLDH) (PDB code 1ldg) involved in glycolysis (or glucose metabolism of the parasite) [52, 53, 54]. There is a strong suggestion that haemoglobin digesting enzymes found in the food vacuole of the plasmodium and pfLDH are potential antimalarial chemotherapeutic targets for chloroquine and related aminoquionlones, anthraquinones and other oxidative phenolic compounds [55, 56, 57, 58, 59, 60]. Besides, chloroquine has been found to bind to the cofactor (NADH) binding site of pfLDH acting as a competitive inhibitor [61].

The binding modes of P2FE-400, a designed inhibitor of plasmepsin II, knipholone, HPMP and chloroquine to plasmepsin II are shown in Figure 4. P2FE-400 showed the highest and strongest affinity for the aspartic protease, plasmepsin II, with the HYDE score of -38.3 kj/mol. The aspartic protease plasmepsin II has two aspartic acid residues Asp34 and Asp214 (the catalytic dyad) that serve as proton donors and acceptors, respectively, in the amide hydrolysis of peptide bonds in proteins. As shown in the current study and also described by Jaudzems *et al*. [62], P2FE-400 forms four hydrogen bonds with the catalytic dyad (Asp34 and Asp214), Val78 and Ser218 amino acid residues. Chloroquine and HPMP showed a comparable binding affinity with an estimated HYDE score of -19.7 and -19.2 kj/mol, respectively. The Cl substituent of chloroquine was found to be unsuitable for binding in the hydrophobic cavity of plasmepsin II. Chloroquine forms hydrogen bonds with Gly36 and Val78 amino acid residues. Similarly, HPMP forms a single hydrogen bond with Ser118. Its methoxyl group and adjacent carbonyl oxygen to the methoxyl group are not favored in the hydrophobic region of the binding pocket. Knipholone and dianellin showed weak binding interaction with HYDE score of -6 and -4.2 kj/mol, respectively. Nonetheless, knipholone forms two hydrogen bonds with one of the catalytic dyad (Asp214) and Val78 amino acid residues.

The binding modes of knipholone, HPMP and chloroquine to pfLDH binding site are shown in Figure 5. Knipholone (-29.1 kj/mol) and HPMP (-26.6kj/mol) showed stronger binding interaction with pfLDH than chloroquine (-26.6kj/mol). Knipholone forms hydrogen bonds with Ile54 and Val98 amino acid residues. Its carbonyl oxygen (at C-9) and hydroxyl group in ring A (at C-1) of the anthraquinone moiety, and the carbonyl oxygen (at C-3¢) of the phloroglucinol moiety together with the *meta* and *para* hydroxyl groups (at C-1¢ and C-4¢) are not favorable for binding. For HPMP, the methoxyl group and double bond in the long aliphatic chain are not suited for binding in the hydrophobic region. It also forms four hydrogen bonds with Ile54, Gly99, Phe100 and Asn140 amino acid residues with unique thermodynamically stable conformation. Interestingly, the two hydrogen bonds that HPMP forms with Gly99 and Asn149 are similar to two of the five hydrogen bond interactions seen in docking of NADH cofactor. From the experimental data, there were seven hydrogen bonds in pfLDH-NADH complex, of which four are observed in this study [63]. Chloroquine on its part showed two hydrogen bonds with Asp53 and Gly99 amino acid residues. One

of the N-ethyl groups of chloroquine is not needed in the hydrophilic binding sites. Moreover, the actual pfLDH-chloroquine complex also showed two hydrogen bonds with Glu122 and Gly99 [61]. In contrast, dianellin did not show binding interaction with pfLDH.

Conclusion

In conclusion, *K. folosia* possesses *in vivo* antimalarial effect against *P. berghei* in mice. This finding in conjunction with the safety profile obtained from the acute oral toxicity results support the traditional claim of the plant for the treatment of malaria. The current molecular docking study also identified the binding motifs of the isolated compounds showing that knipholone and HPMP interact with important amino acid residues in the binding site of the target enzymes.

Abbreviations

AAU: Addis Ababa University; EHNRI: Ethiopian Health Nutrition and Research Institute; HPMP: 12-hydroxypentadec-9-en-1-yl methyl phthalate; ED_{50}: median effective dose; NADH: Nicotinamide adenine dinucleotide; pfLDH: *Plasmodium falciparum* l-lactate dehydrogenase; PTLC: preparative thin layer chromatography; PDB: Protein Data Bank; SoP: School of Pharmacy.

Declarations

Ethics approval and consent to participate

All the animal study procedures followed were reviewed and approved by the Institutional Review Board of the SoP, College of Health Sciences, AAU. The mice were handled were in accordance with the Guide for the Care and Use of Laboratory Animals [20].

Consent for publication

Not applicable

Availability of data and materials

Isolation protocols of the compounds (**1-3**) and their NMR and HRMS spectra are available in the supplementary figures. Tables showing the antimalarial activity of the phenolic fractions and predicting the physicochemical properties of the compounds and summarizing the docking results are available in the supplementary tables.

Competing interests

The authors declare no conflict of interest

Funding

This study was supported by the School of Graduate Studies of Addis Ababa University, research grant.

Authors' contributions

YA conceived the study, collected the plant material, conducted the laboratory experiments and prepared the manuscript. DB and KA were involved in the analysis and interpretation of experimental results, and edited the manuscript. ST run the NMR experiment and edited the manuscript.

Acknowledgements

YA would like to acknowledge the Office of Graduate Studies and Research of Addis Ababa University for the sponsorship. The authors would like to express their gratitude to Professor Sebsebe Demissew, the National Herbarium, Addis Ababa University, for identification of the plant material.

References

1. Cowman AF, Healer J, Marapana D, Marsh K. Malaria: biology and disease. Cell. 2016;167:610–24.
2. WHO. World malaria report 2019. Geneva: World Health Organization; 2019.
3. Snow RW, Sartorius B, Kyalo D, Maina J, Amratia P, Mundia CW, et al. The prevalence of *Plasmodium falciparum* in sub-Saharan Africa since 1900. Nature. 2017;550:515–8.
4. Farooq U, Mahajan RC. Drug resistance in malaria. J Vector Borne Dis. 2004;41:45–53.
5. WHO. World malaria report 2017. Country profile: Ethiopia. Geneva: World Health Organization; 2017.
6. Girum T, Shumbej T, Shewangizaw M. Burden of malaria in Ethiopia, 2000-2016: findings from the Global Health Estimates 2016. Trop Dis Travel Med Vaccines. 2019;5:11.
7. White NJ, Hien TT, Nosten FH. A brief history of Qinghaosu. Trends Parasitol. 2015;31:607–10.
8. Saxena S, Pant N, Jain DC, Bhakuni RS. Antimalarial agents from plant sources. **Curr Sci. 2003;**85:1314–29.
9. Bero J, Frédérich M, Quetin-Leclercq J. Antimalarial compounds isolated from plants used in traditional medicine. J Pharm Pharmacol. 2009;61:1401-33.
10. Ntie-Kang F, Onguéné PA, Lifongo1 LL, Ndom JC, Sippl W, Mbaze LM. The potential of antimalarial compounds derived from African medicinal plants, part II: a pharmacological evaluation of non-alkaloids and non-terpenoids. Malar J. 2014;13:81.
11. Dahlgren RMT, Clifford HT, Yeo PF. The Families of the Monocotyledons. Berlin: Springer-Verlag; 1985.
12. Whitehouse C. Asphodelaceae. In: Beentje HJ, editor. Flora of Tropical East Africa. Roterdam: Balkema Publishers; 2002.
13. Demissew S, Nordan I. Aloes and Lilies of Ethiopia and Eritrea. Addis Ababa: Shama Books; 2010. p. 113-125.

14. Abate G (1989). Etse Debdabe: Ethiopian Traditional Medicine. In: Demissew S, editor. Addis Ababa: Addis Ababa University Press; 1989. p. 99–183.
15. Wube AA, Bucar F, Asres K, Gibbons S, Rattray L, Croft SL. Antimalarial compounds from *Kniphofia foliosa* roots. Phytother Res. 2005;19:472–6.
16. Abdissa N, Akala HM, Heydenreich M, Midiwo JO, Ndakala A, Yenesew A. Knipholone cyclooxanthrone and an anthraquinone dimer with antiplasmodial activities from the roots of *Kniphofia foliosa*. Phytochem Lett. 2013;6:241–5.
17. Endale A, Bisrat D, Animut A, Bucar F, Asres K. *In vivo* antimalarial activity of a labdane diterpenoid from the leaves of *Otostegia integrifolia* Benth. Phytother Res. 2013;27:1805–9.
18. Girma B, Bisrat D, Asres K. Antimalarial evaluation of the leaf latex of *Aloe citrina* and its major constituent. Anc Sci Life. 2015;34:142-6.
19. Teka T, Bisrat D, Yeshak MY, Asres K (2016). Antimalarial activity of the chemical constituents of the leaf latex of *Aloe pulcherrima* Gilbert and Sebsebe. Molecules. 2016;21:1415.
20. National Institute of Health Guidelines for the Care and Use of Laboratory Animals and National Institutes of Health, Office of Science and Health Reports. Guide for care and use of laboratory animals 83-23. Bethesda, Md, USA: Office of Science and Health Reports, Department of Health and Human Services; 1996.
21. OECD. Guidelines for testing of chemicals. Guideline 425: Acute oral toxicity. Paris, France: The Organization of Economic Co-operation and Development; 2008.
22. Waako PJ, Gumede B, Smith P, Folb PI. The *in vitro* and *in vivo* antimalarial activity of *Cardiospermum halicacabum* L. and *Momordica foetida* Schumch. Et Thonn. J Ethnopharmacol. 2005;99:137–43.
23. Hilou A, Nacoulma OG, Guiguemde TR. *In vivo* antimalarial activities of extracts from *Amaranthus spinosus* L. and *Boerhaavia erecta* L. in mice. J Ethnopharmacol. 2006;103:236–40.
24. Ancelin ML, Calas ML, Bonhoure A, Herbute S, Vial HJ. *In vivo* antimalarial activities of mono-and bis quaternary ammonium salts interfering with *Plasmodium* phospholipid metabolism. Antimicrob Agents Chemother. 2003;47:2598–05.
25. Vennerstrom JL, Arbe-Barnes S, Brun R, Charman SA, Chiu FCK, Chollet J, et al. Identification of an antimalarial synthetic trioxolane drug development candidate. Nature. 2004;430:900-4.
26. Fentahun S, Makonnen E, Awas T, Giday M. *In vivo* antimalarial activity of crude extracts and solvent fractions of leaves of *Strychnos mitis* in *Plasmodium berghei* infected mice. BMC Complement Altern Med. 2017;17:13.
27. Schneider N, Hindle S, Lange G, Klein R, Albrecht J, Briem H, et al. Substantial improvements in large-scale redocking and screening using the novel HYDE scoring function. J Comput Aided Mol Des. 2012;26:701–23.
28. Schneider N, Lange G, Hindle S, Klein R, Rarey M. A consistent description of Hydrogen bond and dehydration energies in protein–ligand complexes: methods behind the HYDE scoring function. J Comput Aided Mol Des. 2013;27:15-29.

29. Cichewicz RH, Nair MG. Isolation and characterization of stelladerol, a new antioxidant naphthalene glycoside, and other antioxidant glycosides from edible daylily (*Hemerocallis*) flowers. J Agric Food Chem. 2002;50:87–91.
30. Dias DA, Silva CA, Urban S. Naphthalene aglycones and glycosides from the Australian medicinal plant, *Dianella callicarpa*. Planta Med. 2009;75:1442–7.
31. Cichewicz RH, Lim K-C, McKerrow JH, Nair MG. Kwanzoquinones A – G and other constituents of *Hemerocallis fulva* 'Kwanzo' roots and their activity against the human pathogenic trematode *Schistosoma mansoni*. Tetrahedron. 2002;58:8597–06.
32. Bezabih M, Abegaz BM. 4'-Demethyl knipholone from aerial parts of *Bulbine capitata*. Phytochemistry. 1998;48:1071-3.
33. Dagne E, Steglich W. Knipholone: a unique anthraquinone derivative from *Kniphofia foliosa*. Phytochemistry. 1984;23:1729-31.
34. Amade P, Mallea M, Bouaicha N. Isolation, structural identification and biological activity of two metabolites produced by *Penicillium olsonii* Bainier and Sartory. J Antibiot (Tokyo). 1994;47:201-7.
35. Sastry VMVS, Rao GRK. Dioctyl phthalate, and antibacterial compound from the marine brown alga—*Sargassum wightii.* J Appl Phycol. 1995;7:185-6.
36. Lee KH, Hong HS, lee CH. Induction of apoptosis in human leukaemic cell lines K562, HL60 and U937 by diethylhexylphthalate isolated from *Aloe vera* Linne. J Pharm Pharmacol. 2000;52:1037-41.
37. Chatterjee S, Dutta TK. Metabolism of butyl benzyl phthalate by *Gordonia* sp. strain MTCC 4818. Biochem Biophys Res Commun. 2003;309:36–43.
38. Geremedhin G, Bisrat D, Asres K. Isolation, characterization and *in vivo* antimalarial evaluation of anthrones from the leaf latex of *Aloe percrassa* Todaro. J Nat Remedies. 2014;14:119-25.
39. Deharo E, Bourdy G, Quenevo C, Muñoz V, Ruiz G, Sauvain M. A search for natural bioactive compounds in Bolivia through a multidisciplinary approach. Part V. Evaluation of the antimalarial activity of plants used by the Tacana Indians. J Ethnopharmacol. 2001;77:91–8.
40. Abosi AO, Raseroka BH. *In vivo* antimalarial activity of *Vernonia amygdalina.* Br J Biomed Sci. 2003;60:89-91.
41. Kaou AM, Mahiou-Leddet V, Hutter S, Aïnouddine S, Hassani S, Yahaya I, et al. Antimalarial activity of crude extracts from nine African medicinal plants. J Ethnopharmacol. 2008;116:74–83.
42. Liu Y, Murakami N, Ji H, Abreu P, Zhang S. Antimalarial flavonol glycosides from *Euphorbia hirta*. Pharm Biol. 2007;45:278–81.
43. Bankole AE, Adekunlel AA, Sowemimo AA, Umebese CE, Abiodun O, Gbotosho GO. Phytochemical screening and *in vivo* antimalarial activity of extracts from three medicinal plants used in malaria treatment in Nigeria. Parasitol Res. 2016;115:299-05.
44. Alson SG, Jansen O, Cieckiewicz E, Rakotoarimanana H, Rafatro H, Degotte G, et al. *In vitro* and *in vivo* antimalarial activity of caffeic acid and some of its derivatives. J Pharm Pharmacol. 2018;70:1349-56.

45. Winter RW, Cornell KA, Johnson LL, Ignatushchenko MV, Hinrichs DJ, Riscoe MK. Potentiation of the antimalarial agent rufigallol. Antimicrob Agents Chemother. 1996;40:1408–11.
46. Hernández-Medel MR, Pereda-Miranda R. Cytotoxic anthraquinone derivatives from *Picramnia antidesma*. Planta Med. 2002;68:556-8.
47. François G, Steenackers T, Assi LA, Steglich W, Lamottke K, Holenz J, et al. Vismione H and structurally related anthranoid compounds of natural and synthetic origin as promising drugs against the human malaria parasite *Plasmodium falciparum*: structure-activity relationships. Parasitol Res. 1999;85:582-8.
48. Ignatushchenkoa MV, Winter RW, Bächinger HP, Hinrichs DJ, Riscoe MK. Xanthones as antimalarial agents; studies of a possible mode of action. FEBS Lett. 1997;409:67-73.
49. Ziegler J, Linck R, Wright DW. Heme aggregation inhibitors: antimalarial drugs targeting an essential biomineralization process. Curr Med Chem. 2001;8:171–89.
50. Kutner S, Breuer WV, Ginsburg H, Cabantchik ZI. On the mode of action of phlorizin as an antimalarial agent in *in vitro* cultures of *Plasmodium falciparum.* Biochem Pharmacol. 1987;36:123-9.
51. Ehrenkranz JRL, Lewis NG, Kahn CR, Roth J. Phlorizin: a review. Diabetes Metab Res Rev. 2005;21:31–8.
52. Bazik DJ, Fox BA, Gonyer K. Expression of *Plasmodium falciparum* lactate dehydrogenase in *Escherichia coli.* Mol Biochem Parasitol. 1993;59:155-66.
53. Silva AM, Lee AY, Gulnik SV, Majer P, Collins J, Bhat TN, et al. Structure and inhibition of plasmepsin II, a hemoglobin-degrading enzyme from *Plasmodium falciparum*. Proc Natl Acad Sci USA. 1996;93:10034–9.
54. Nöteberg D, Hamelink E, Hultén J, Wahlgren M, Vrang L, Samuelsson B, et al. Design and synthesis of plasmepsin I and plasmepsin II inhibitors with activity in *Plasmodium falciparum*-infected cultured human erythrocytes. J Med Chem. 2003;46:734-46.
55. Slater AF (1993). Chloroquine: mechanism of drug action and resistance in *Plasmodium falciparum.* Pharmacol Ther. 1993;57:203-35.
56. Haque TS, Skillman AG, Lee CE, Habashita H, Gluzman IY, Ewing TJA, et al. Potent, low-molecular-weight non-peptide inhibitors of malarial aspartyl protease plasmepsin II. J Med Chem. 1999;42:1428-40.
57. Choi SR, Pradhan A, Hammond NL, Chittiboyina AG, Tekwani BL, Avery MA. Design, synthesis, and biological evaluation of *Plasmodium falciparum* lactate dehydrogenase inhibitors. J Med Chem. 2007;50:3841-50.
58. D'Alessandro S, Silvestrini F, Dechering K, Corbett Y, Parapini S, Timmerman M, et al. A *Plasmodium falciparum* screening assay for anti-gametocyte drugs based on parasite lactate dehydrogenase detection. J Antimicrob Chemother. 2013;68:2048-58.
59. Tiwari HK, Kumar P, Jatana N, Kumar K, Garg S, Narayanan L, et al. *In vitro* antimalarial evaluation of piperidine- and piperazine-based chalcones: inhibition of falcipain-2 and plasmepsin II hemoglobinases activities from *Plasmodium falciparum*. ChemistrySelect. 2017;2:7684–90.

60. Cheuka PM, Dziwornu G, Okombo J, Chibale K. Plasmepsin inhibitors in antimalarial drug discovery: medicinal chemistry and target validation (2000 to present). J Med Chem. 2010;63:4445–67.
61. Read JA, Wilkinson KW, Tranter R, Sessions RB, Brady RL. Chloroquine binds in the cofactor binding site of *Plasmodium falciparum* lactate dehydrogenase. J Biol Chem. 1999;274:10213–8.
62. Jaudzems K, Tars K, Maurops G, Ivdra N, Otikovs M, Leitans J, et al. Plasmepsin inhibitory activity and structure-guided optimization of a potent hydroxyethylamine-based antimalarial hit. ACS Med Chem Lett. 2014;5:373–7.
63. Chaikuad A, Fairweather V, Conners R, Joseph-Horne T, Turgut-Balik D, Brady RL. Structure of lactate dehydrogenase from *Plasmodium* v*ivax*: complexes with NADH and APADH. Biochemistry. 2005;44:16221-8.

Figures

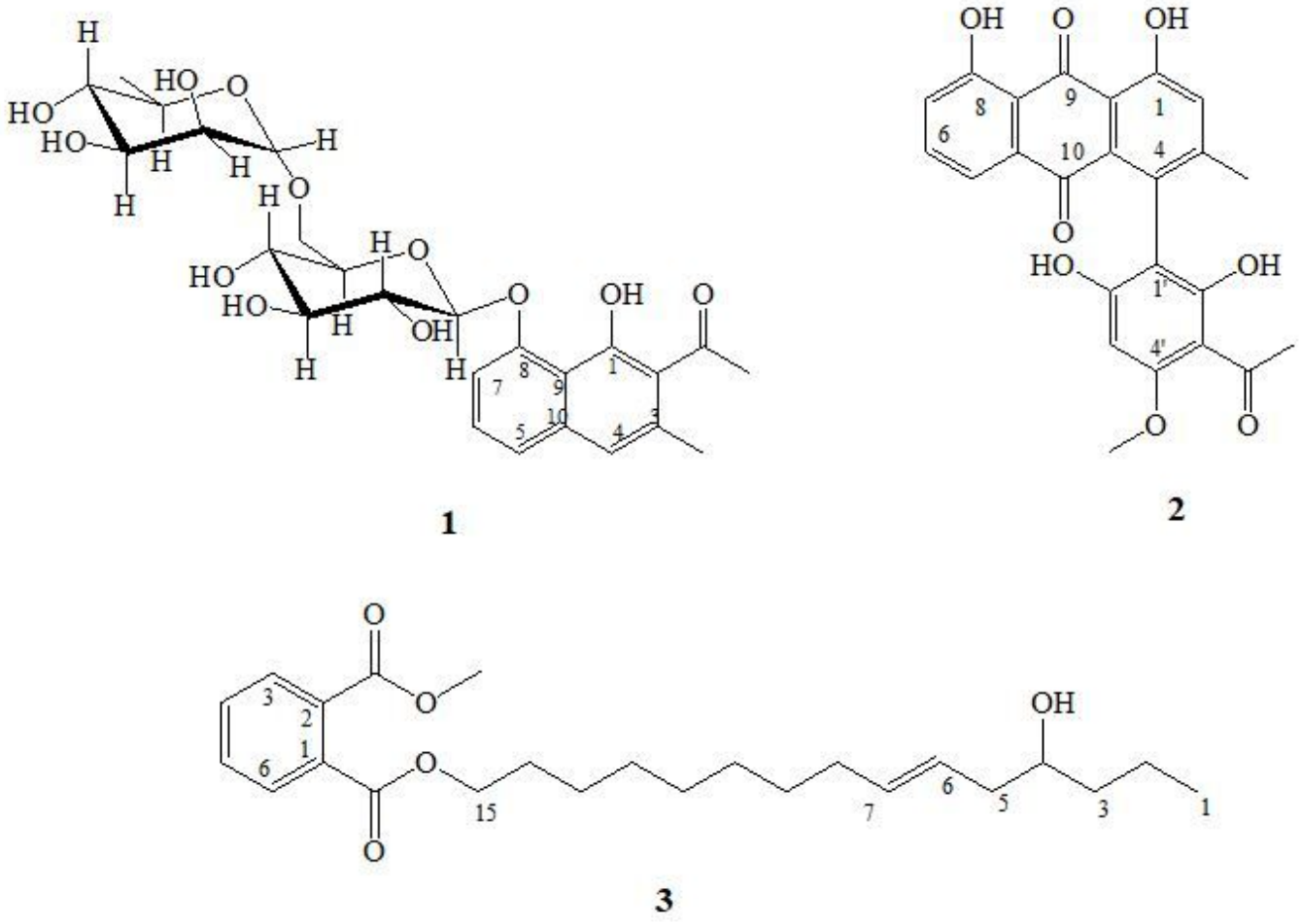

Figure 1

Chemical structures of dianellin (1), knipholone (2) and 12-hydroxypentadec-9-en-1-yl methyl phthalate (3).

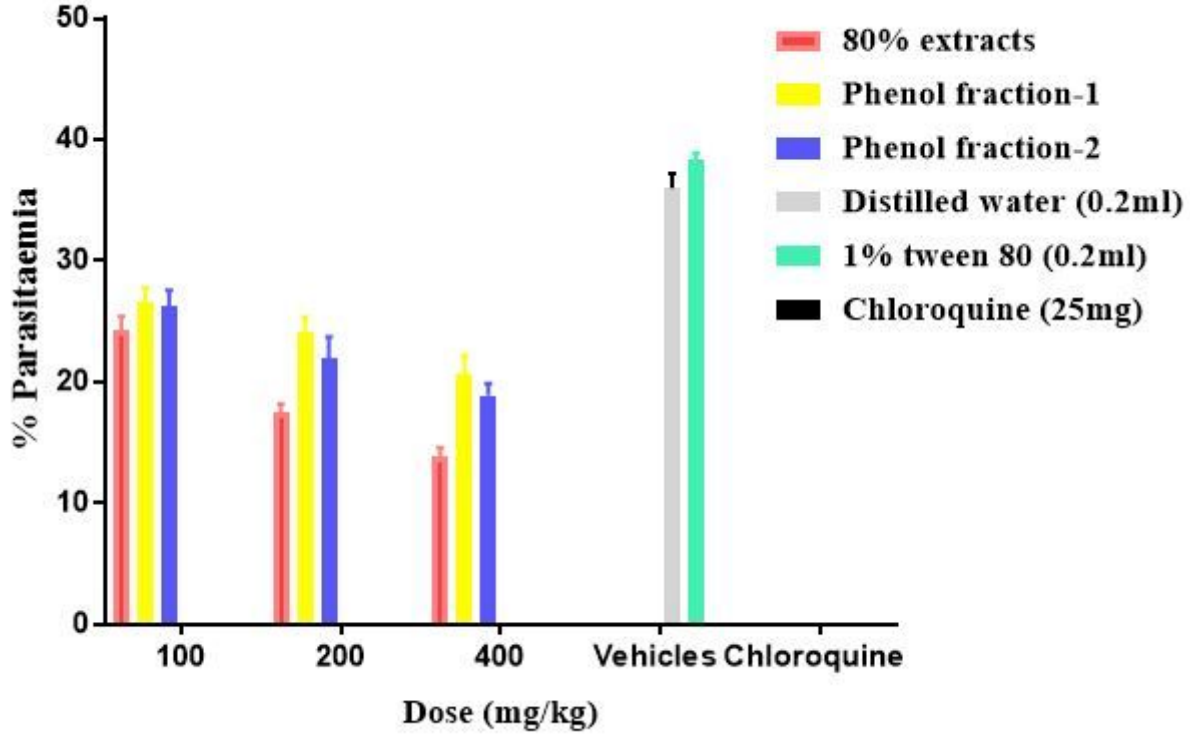

Figure 2

Antimalarial activity of the 80% extract and phenol fractions of K. folosiain mice infected with Plasmodium bergheiin 4 day suppression test.Values are presented as mean ± SEM; n =5.

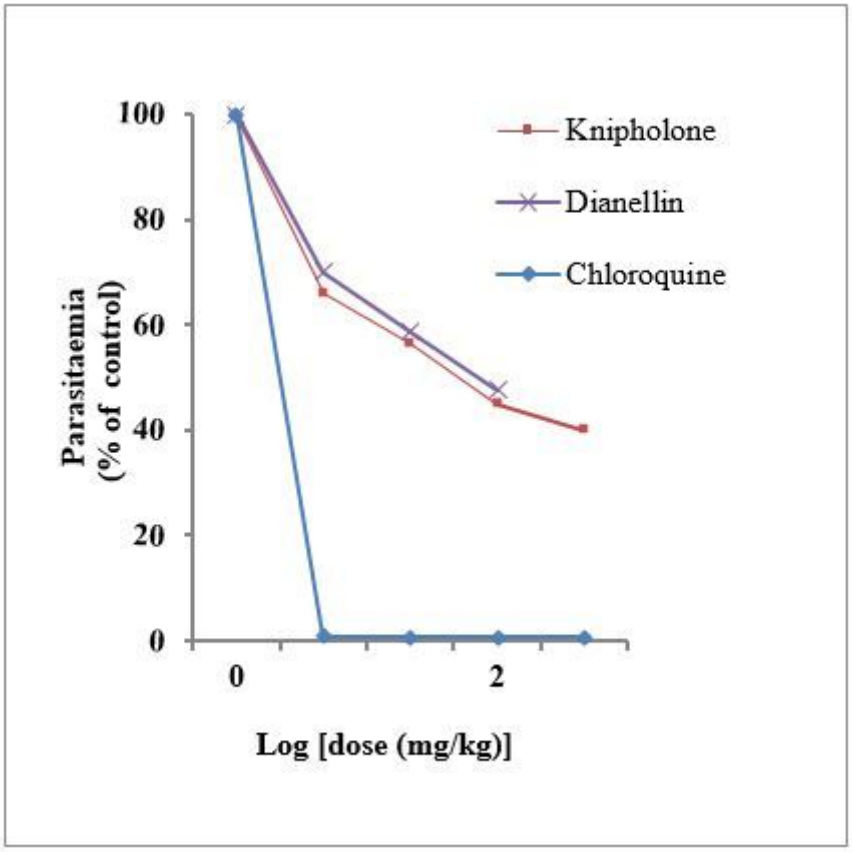

Figure 3

Antimalarial activity of knipholone and dianellin in mice infected with Plasmodium berghei. The ED50 was estimated from a plot of log dose against parasitaemia (expressed as a percentage of the control). Values are presented as mean ± SEM; n =5.

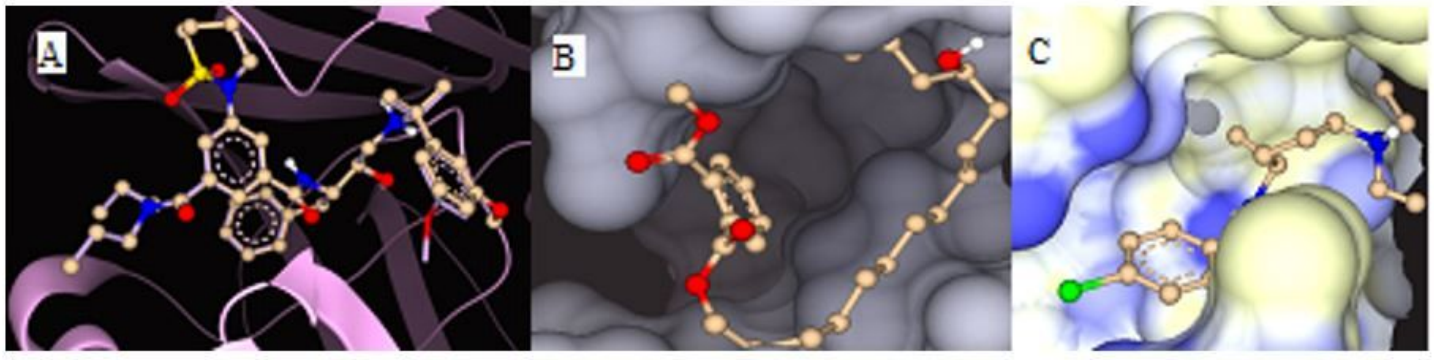

Figure 4

A) Superimposition of redocked P2FE-400 (shown as a solid line) with its original position (shown in ball-stick model) as a complex (co-crystal) in the binding site of the crystal structure of plasmepsin II (PDB 4cku). B) Surface representation showing HPMP in the binding site of plasmepsin II. HPMP is shown in ball-stick model. C) Surface representation showing chloroquine in the binding site of plasmepsin II with

lipophilicity coloring, white representing hydrophobic pockets and blue representing hydrophilic pockets. Chloroquine is shown in ball-stick model.

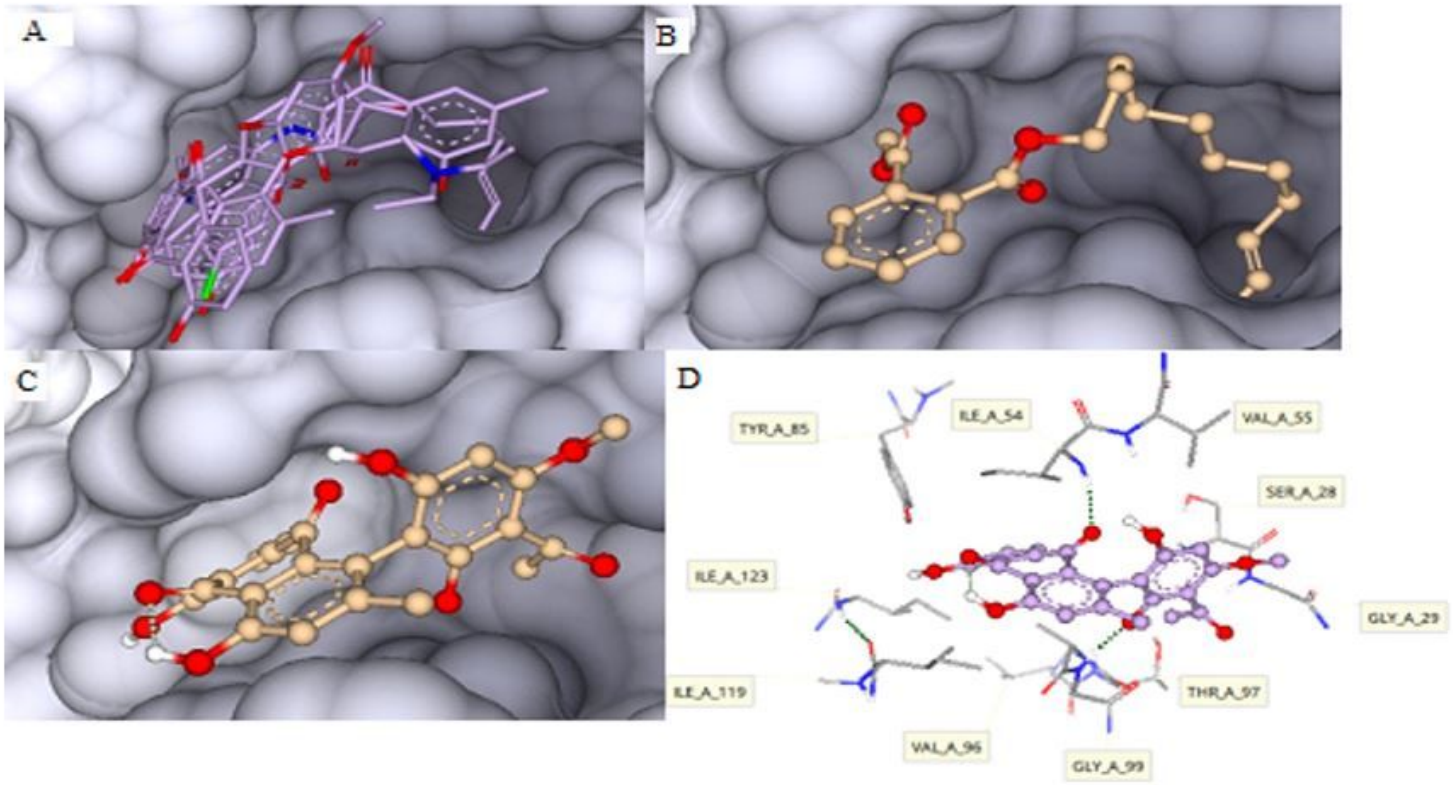

Figure 5

A) Surface representation showing the superimposed compounds in the binding site of plasmodium falciparum l-lactate dehydrogenase (pfLDH) (PDB1ldg). B) Surface representation showing HPMP in the binding site of pfLDH. HPMP is shown in ball-stick model. C) Surface representation showing knipholone in the binding site of pfLDH. Knipholone is shown in ball-stick model. D) Binding interaction of knipholone with amino acid residues of pfLDH.

Supplementary Files

This is a list of supplementary files associated with this preprint. Click to download.

- SupplementarymaterialsMJ.docx